Chart I

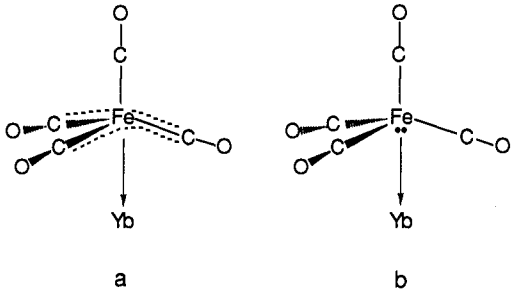

consists of "polymeric ladders" extending along the crystallographic *b* axis of the lattice. There are two crystallographically independent ladders, and they are stereochemically similar. Figure 1 shows a portion of one ladder. The local coordination geometries for the Fe and Yb atoms are shown in Figure 2. The geometries of the $[Fe(CO)_4]^{2-}$ units in **2** are intermediate between a tetrahedron and a trigonal bipyramid, while those of the Yb^{2+} ions are distorted octahedrons. In addition to three CH_3CN ligands, each Yb^{2+} ion is coordinated by two carbonyl oxygens from two different $Fe(CO)_4$ units; and each $Fe(CO)_4$ unit is in turn connected to two different Yb^{2+} ions via isocarbonyl linkages, thus forming a zigzag ···Yb-O-C-Fe-C-O-Yb··· chain. Two such chains are coupled to form a ladder through Yb-Fe interactions.[11] Two independent Yb-Fe distances are 3.012 (1) Å and 3.009 (1) Å. These distances are comparable to a Yb-Fe distance of 3.00 Å in $YbFe_2$ alloy,[12] and shorter than the sum of Yb and Fe metallic radii (3.2 Å).[13] Long Yb···C contacts are observed at 3.026 (9), 3.073 (8), and 3.201 (9) Å for Yb···Cl, Yb···C2, and Yb···C3, respectively (Figure 2). Metal-metal distances in several oligomeric $Fe(CO)_4$-containing complexes are cited here for comparison. The average bond distances of 2.56 (4) Å for Zn-Fe in $[(bpy)ZnFe(CO)_4]_2$,[14] 2.562 (3) Å for Cd-Fe in $[CdFe(CO)_4]_4 \cdot 2C_3H_6O$,[15] and 2.640 (7) Å for Cd-Fe in $[(bpy)CdFe(CO)_4]_3 \cdot {}^3/_4C_6H_3Cl_3$[16] are 0.07, 0.22, and 0.14 Å shorter than the sums of their respective metallic radii.[13]

The Yb-Fe interaction in **2** can be described as a dative bond formed by electron-pair donation from the Fe center in $[Fe(CO)_4]^{2-}$ to Yb^{2+}, similar to a Ru-Th dative bond in $Cp^*_2(I)ThRuCp(CO)_2$.[1f] The Yb···C contact distances of over 3 Å and the fact that the carbonyl groups are nearly linear (the Fe-C-O angles average 177.0 [1.4]° [20b]) suggest that there are only weak interactions between the Yb^{2+} ions and three carbonyl carbons. Therefore, any contribution due to the trimethylenemethane-like coordination of the FeC_3 region of $[Fe(CO)_4]^{2-}$ to Yb^{2+} (Chart Ia) is less significant than that of the direct Yb-Fe bonding (Chart Ib). This conclusion is further supported by comparison of the structural data of **2** with that of $Na_2[Fe(CO)_4] \cdot 1.5(C_4H_8O_2)$.[17] In the latter, an allyl-like interaction between the Na^+ ions and the C-Fe-C regions of $[Fe(CO)_4]^{2-}$ was proposed. Note that six-coordinate Na^+ and Yb^{2+} have the same ionic radii of 1.02 Å.[18] In $Na_2[Fe(CO)_4] \cdot 1.5(C_4H_8O_2)$ the Na···Fe distance of 3.086 (2) is longer than two Na···C distances of 2.860 (5) and 3.050 (5) Å, while in **2** the Yb-Fe distances are shorter than the Yb···C distances.

The average Yb-N bond distance of 2.515 [18] Å in **2** is comparable to the Yb-N bond distances in $(CH_3CN)_4Yb[(\mu\text{-}H)_3BH]_2$[19b] and $(CH_3CN)_6Yb(\mu\text{-}H)_2B_{10}H_{12}$[19a] (2.525 [6] and 2.55 [3] Å, respectively). The average Yb-O bond distance for the Yb-isocarbonyl linkages in **2** is 2.374 [7] Å, ca. 0.1 Å longer than those involving eight-coordinate trivalent Yb ions.[6] For the carbonyls involved in the isocarbonyl linkages, the average C-O bond distance of 1.195 [7] Å and the average Fe-C bond distance of 1.726 [9] Å suggest the weakening of the C-O bonds and the strengthening of the Fe-C bonds upon isocarbonyl coordination to Yb^{2+}.[6] The average C-O and Fe-C bond distances for the terminal carbonyls are 1.154 [9] and 1.768 [11] Å, respectively. The Yb-N-C angles vary from 140.0 (7) to 170.8 (7)°, and the Yb-O-C angles vary from 134.8 (5) to 168.4 (5)°. The angularity of the Yb-O-C and Yb-N-CCH_3 interactions in **2** is probably controlled by steric effects.

Presently we are developing the chemistry of this system and extending our procedures to additional examples of metal-metal interactions involving lanthanides and transition metals.

Acknowledgment. This work was supported by the National Science Foundation through Grant CHE88-00515.

Supplementary Material Available: Listings of positional parameters, anisotropic thermal parameters, bond distances, and bond angles of **2**, a brief description of the crystal structure of **2**, and a stereoview of the crystal packing diagram of the unit cell of **2** (11 pages); listing of calculated and observed structure factor amplitudes for **2** (19 pages). Ordering information is given on any current masthead page.

(11) The difference Fourier map gives no evidence of residual electron density that can be assigned to a hydrogen bridging Yb and Fe. This is consistent with the infrared spectrum of **2**, which suggests the presence of distorted $[Fe(CO)_4]^{2-}$ instead of $[HFe(CO)_4]^-$. For infrared spectra of $[Fe(CO)_4]^{2-}$ and $[HFe(CO)_4]^-$, see ref 9 and the following: Mitsudo, T.; Watanabe, Y.; Yamashita, M.; Takegami, Y. *Chem. Lett.* **1974**, 1385.

(12) Cannon, J. F.; Robertson, D. L.; Hall, H. T. *Mater. Res. Bull.* **1972**, *7*, 5.

(13) Wells, A. F. *Structural Inorganic Chemistry*, 5th ed.; Oxford University Press: New York, 1984; p 1288.

(14) Neustadt, R. J.; Cymbaluk, T. H.; Ernst, R. D.; Cagle, F. W., Jr. *Inorg. Chem.* **1980**, *19*, 2375.

(15) Ernst, R. D.; Marks, T. J.; Ibers, J. A. *J. Am. Chem. Soc.* **1977**, *99*, 2090.

(16) Ernst, R. D.; Marks, T. J.; Ibers, J. A. *J. Am. Chem. Soc.* **1977**, *99*, 2098.

(17) (a) Chin, H. B.; Bau, R. *J. Am. Chem. Soc.* **1976**, *98*, 2434. (b) Teller, R. G.; Finke, R. G.; Collman, J. P.; Chin, H. B.; Bau, R. *J. Am. Chem. Soc.* **1977**, *99*, 1104.

(18) Shannon, R. D. *Acta Crystallogr.* **1976**, *A32*, 751.

(19) (a) White, J. P., III; Deng, H.; Shore, S. G. *J. Am. Chem. Soc.* **1989**, *111*, 8946. (b) White, J. P., III; Deng, H.; Shore, S. G. *Inorg. Chem.* **1991**, *30*, 2337.

(20) (a) The specific distance or angle given for **2** is the average of two crystallographically independent values, with estimated standard deviation $s = (s_1 + s_2)^{1/2}$ shown in parentheses. (b) The average distance or angle is the mean of several values, and the esd shown in brackets is calculated from $[\sum_{i=1}^{N}(d_i - \bar{d})^2/(N-1)]^{1/2}$, where d_i is the ith value and $\bar{d}$ is the mean of N values.

Photoinduced Electron Transfer in Redox-Active Lysines

Sandra L. Mecklenburg, Brian M. Peek,
Bruce W. Erickson,* and Thomas J. Meyer*

Department of Chemistry, University of North Carolina
Chapel Hill, North Carolina 27599-3290

Received March 14, 1991
Revised Manuscript Received August 20, 1991

Intramolecular photoinduced redox separation in molecules incorporating both an electron transfer donor and an acceptor as well as a chromophore has previously been achieved in carotenoid porphyrin-quinones,[1] aniline porphyrin-quinones,[2] and ruthenium

(1) (a) Gust, D.; Moore, T. A.; Moore, A. L.; et al. *J. Am. Chem. Soc.* **1991**, *113*, 3638. (b) Gust, D.; Moore, T. A.; Moore, A. L.; Lee, S.-J.; Bittersmann, E.; Luttrull, D. K.; Rehms, A. A.; DeGraziano, J. M.; Ma, X. C.; Gao, F.; Belford, R. E.; Trier, T. T. *Science* **1990**, *248*, 199. (c) Gust, D.; Moore, T. A. *Science* **1989**, *244*, 35. (d) Gust, D.; Moore, T. A.; Moore, A. L.; Makings, L. R.; Seely, G. R.; Ma, X.; Trier, T. T.; Gao, F. *J. Am. Chem. Soc.* **1988**, *110*, 7567. (e) Moore, T. A.; Gust, D.; Mathis, P.; Mialoccq, J.-C.; Chachaty, C.; Bennsasson, R. V.; Band, E. J.; Doizi, D.; Liddell, P. A.; Lehman, W. R.; Nemeth, G. A.; Moore, A. L. *Nature* **1984**, *307*, 630.

(2) (a) Wasielewski, M. R.; Gaines, G. L., III; O'Neil, M. P.; Svec, W. A.; Niemczyk, M. P. *J. Am. Chem. Soc.* **1990**, *112*, 4559. (b) Hofstra, U.; Schaafsma, T. J.; Sanders, G. M.; Van Dijk, M.; Van Der Plas, H. C.; Johnson, D. G.; Wasielewski, M. R. *Chem. Phys. Lett.* **1988**, *151*, 169. (c) Schmidt, J. A.; McIntosh, A. R.; Weedon, A. C.; Bolton, J. R.; Connolly, J. S.; Hurley, J. K.; Wasielewski, M. R. *J. Am. Chem. Soc.* **1988**, *110*, 1733. (d) Wasielewski, M. R.; Niemczyk, M. P.; Svec, W.; Pewitt, E. B. *J. Am. Chem. Soc.* **1985**, *107*, 5562.

0002-7863/91/1513-8540$02.50/0

Scheme I

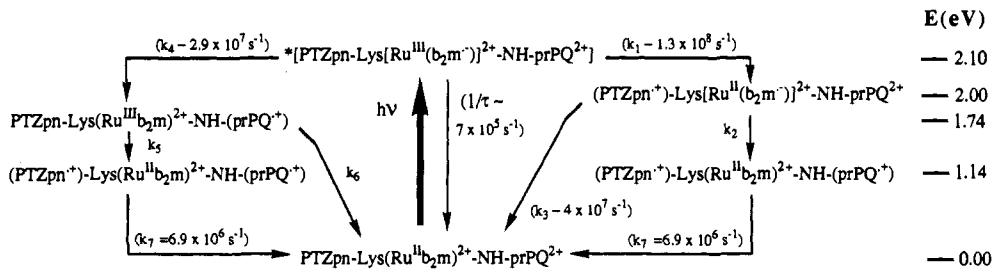

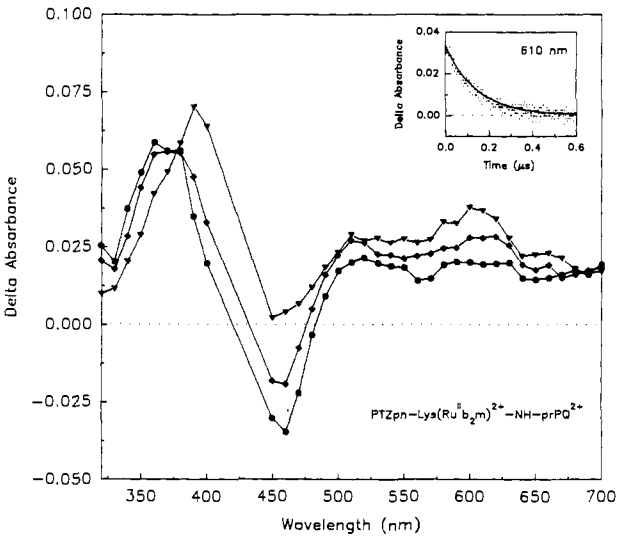

Figure 1. Transient absorption difference spectra obtained following 420-nm, 6-ns pulsed (≤5.2 mJ/pulse) excitation of [PTZpn-Lys-$(Ru^{II}b_2m)^{2+}$-NH-prPQ^{2+}] in argon-bubbled CH_3CN at 25 °C: 20 ns (circles), 25 ns (diamonds), and 45 ns (triangles) after the excitation pulse. Inset: Typical fitted decay trace for data obtained at 610 nm. The experimental data points are represented by the dots; the solid curve is the fit to a single-exponential function with a rate constant of k = (6.9 ± 0.2) × 10^6 s^{-1} (τ = 146 ± 3 ns).

polypyridyl complexes.[3] The secondary structures of peptides have been exploited as a means of providing controlled orientation or spacing of photoactive sites in studies of intramolecular electron transfer.[4-6] We have attempted to combine these two concepts and report here the first example of a redox-active assembly in which a single amino acid has been functionalized via amide bonds with an electron-transfer donor, a chromophore, and an electron-transfer acceptor. The assembly exhibits photoinduced, spatially directed redox separation, which is achieved through a series of single electron transfer events. Our observations establish the feasibility of utilizing similar synthetic amino acids to construct peptides in which controlled spatial arrays of chromophores, donors, and acceptors may allow optimization in the formation and persistence of redox-separated states.

We adopted a modular approach based on a trifunctionalized amino acid to prepare the PF_6^- salt of the chromophore-quencher triad shown below, [PTZpn-Lys$(Ru^{II}b_2m)^{2+}$-NH-prPQ^{2+}]$(PF_6)_4$.[7]

Derivatives of the chromophore $(Ru^{II}b_3)^{2+}$, the donor PTZ, and the acceptor PQ^{2+} were prepared[8] and attached stepwise to the functional groups of L-lysine. Also prepared were the model chromophore [$(Ru^{II}b_2m)^{2+}$-NH-CH_3]$(PF_6)_2$ and two model dyads, [PTZpn-Lys$(Ru^{II}b_2m)^{2+}$-OCH_3]$(PF_6)_2$ and [Boc-Lys-$(Ru^{II}b_2m)^{2+}$-NH-prPQ^{2+}]$(PF_6)_4$, where the NH-prPQ^{2+} group of the triad was replaced by methoxy or the PTZpn group by *tert*-butoxycarbonyl (Boc), respectively. Each compound was purified by cation-exchange HPLC and characterized by mass and ^1H NMR spectrometry and by UV–visible absorption spectroscopy.[9]

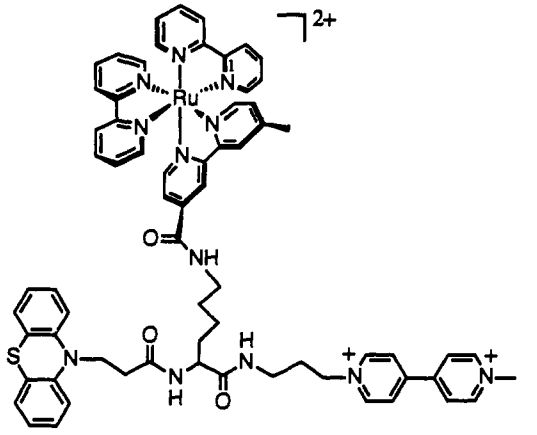

[PTZpn-Lys$(Ru^{II}b_2m)^{2+}$-NH-prPQ^{2+}]

For all four complexes, a characteristic $d\pi(Ru^{II}) \rightarrow \pi^*$(b,m) metal-to-ligand charge transfer (MLCT) absorption was observed at 458 nm. Emission from [$(Ru^{II}b_2m)^{2+}$-NH-CH_3] occurred with λ_{max} = 645 nm, a quantum yield of 0.087 ± 0.001, and a lifetime of 1380 ns in CH_3CN. With the attached electron transfer donor and/or acceptor, the emission was largely quenched. For [Boc-Lys$(Ru^{II}b_2m)^{2+}$-NH-prPQ^{2+}], Φ_{em} = 0.003 ± 0.001 and τ_{650} = 40 ± 4 ns; for [PTZpn-Lys$(Ru^{II}b_2m)^{2+}$-OCH_3], Φ_{em} = 0.003 ± 0.001 and τ_{645} = 14 ± 4 ns. A weak, residual emission observed from [PTZpn-Lys$(Ru^{II}b_2m)^{2+}$-NH-prPQ^{2+}], Φ_{em} = 0.004 ± 0.001, τ_{645} = 18 ± 4 ns, appears to be due to a dyad impurity.

Nanosecond, time-resolved absorption spectroscopy[10] of [PTZpn-Lys$(Ru^{II}b_2m)^{2+}$-NH-prPQ^{2+}] revealed that the origin of the emission quenching is electron transfer between the excited chromophore and the donor and acceptor, as outlined in Scheme I. Transient absorption difference spectra of the lysine triad in

(3) (a) Worl, L. A.; Strouse, G. F.; Younathan, J. N.; Baxter, S. M.; Meyer, T. J. *J. Am. Chem. Soc.* **1990**, *112*, 7571. (b) Meyer, T. J. *Acc. Chem. Res.* **1989**, *22*, 163. (c) Strouse, G. F.; Worl, L. A.; Younathan, J. N.; Meyer, T. J. *J. Am. Chem. Soc.* **1989**, *111*, 9101. (d) Danielson, E.; Elliott, C. M.; Merkert, J. W.; Meyer, T. J. *J. Am. Chem. Soc.* **1987**, *109*, 2519. (e) Olmsted, J., III; McClanahan, S. F.; Danielson, E.; Younathan, J. N.; Meyer, T. J. *J. Am. Chem. Soc.* **1987**, *109*, 3297. (f) Margerum, L. D.; Murray, R. W.; Meyer, T. J. *J. Phys. Chem.* **1986**, *90*, 728.

(4) (a) Inai, Y.; Sisido, M.; Imanishi, Y. *J. Phys. Chem.* **1991**, *95*, 3847. (b) Sisido, M.; Tanaka, R.; Inai, Y.; Imanishi, Y. *J. Am. Chem. Soc.* **1989**, *111*, 6790.

(5) Schanze, K. S.; Sauer, K. *J. Am. Chem. Soc.* **1988**, *110*, 1180.

(6) (a) Vassilian, A.; Wishart, J. F.; van Hemelryck, B.; Schwarz, H.; Isied, S. S. *J. Am. Chem. Soc.* **1990**, *112*, 7278. (b) Isied, S. S.; Vassilian, A.; Magnuson, R. H.; Schwarz, H. A. *J. Am. Chem. Soc.* **1985**, *107*, 7432.

(7) Abbreviations: b = 2,2′-bipyridine; Boc = *tert*-butoxycarbonyl; BQ = 1,4-benzoquinone; Lys = L-lysine; m = 4′-methyl-2,2′-bipyridine-4-carbonyl; PTZ = 10*H*-phenothiazine; PTZpn = 3-(10*H*-phenothiazine-10)propanoyl; PQ^{2+} = paraquat (1,1′-dimethyl-4,4′-bipyridinium); prPQ^{2+} = 3-(1′-methyl-4,4′-bipyridinium)propyl; and TMBD = *N,N,N′,N′*-tetramethylbenzidine.

(8) Peek, B. M.; Ross, G. T.; Edwards, S. W.; Meyer, G. J.; Meyer, T. J.; Erickson, B. W. *Int. J. Pept. Protein Res.* **1991**, *38*, 114.

(9) (a) Peek, B. M. Ph.D. Dissertation, University of North Carolina at Chapel Hill, 1991. (b) Peek, B. M.; Edwards, S. W.; Mecklenburg, S. L.; Meyer, T. J.; Erickson, B. W., manuscript in preparation including full details of the syntheses and characterization of the compounds. (c) Characterization data are included here as supplementary material.

(10) (a) Duesing, R.; Tapolsky, G.; Meyer, T. J. *J. Am. Chem. Soc.* **1990**, *112*, 5378. (b) Danielson, E., in preparation.

argon-bubbled CH_3CN acquired at various times after excitation with a 420-nm, 6-ns laser pulse (≤5.2 mJ/pulse) are shown in Figure 1. The spectra are corrected for emission. At 20 ns after the excitation pulse, increased absorbance at 370 nm due to the bipyridyl anion radical and bleaching at 440–460 nm due to the loss of the ground-state, $d\pi(Ru^{II}) \rightarrow \pi^*(b,m)$ transition were observed, in addition to absorptions in the 490–690-nm region. At later times, the 370-nm absorption shifted to 390 nm, the bleaching disappeared, and absorptions in the visible region increased in intensity with maxima at 510 and 610 nm. The band at 510 nm is due to $PTZpn^{\bullet+}$,[11] while the bands at 390 and 610 nm are due to $prPQ^{\bullet+}$.[12] By 45 ns after the pulse, the difference spectrum corresponded to a superposition of the spectra of $PTZpn^{\bullet+}$ and $prPQ^{\bullet+}$, consistent with the formation of the redox-separated state, $[(PTZpn^{\bullet+})\text{-}Lys(Ru^{II}b_2m)^{2+}\text{-}NH\text{-}(prPQ^{\bullet+})]$. The maximum absorbance increase at 610 nm occurred 45 ns after the excitation pulse, after which the difference spectrum decayed monoexponentially to the base line with a lifetime of 146 ± 3 ns ($k_7 = 6.9 \pm 0.2 \times 10^6\ s^{-1}$). The observed monoexponential decay implies that a single conformation of the triad predominates in solution or, more likely, that the conformational equilibria which exist for the interconversion between conformers are rapid on the time scale of the electron transfer. The energy stored in the redox-separated state was 1.14 V, based on the measured redox potentials of the donor and acceptor of the triad.

Analysis of transient absorption and emission data for the model dyads allows us to assign values to some of the rate constants in Scheme I. The rate constant for the appearance of $PTZpn^{\bullet+}$ in the triad, $k_1 = 1.3 \times 10^8\ s^{-1}$, was the same within experimental error as that obtained for quenching of the MLCT excited state in the dyad $[PTZpn\text{-}Lys(Ru^{II}b_2m)^{2+}\text{-}OCH_3]$, based on analysis of rise-time kinetics monitored at 510 nm. The appearance of $prPQ^{\bullet+}$ in the triad occurs with a rate constant indistinguishable from that for the appearance of $PTZpn^{\bullet+}$. This is more rapid than MLCT quenching in the dyad $[Boc\text{-}Lys(Ru^{II}b_2m)^{2+}\text{-}NH\text{-}prPQ^{2+}]$, $k = 3 \times 10^7\ s^{-1}$. From the ratio of rate constants for the models it can be inferred that $k_4/k_1 \sim 0.2$, indicating that the left-hand branch makes a relatively small contribution to excited-state quenching. We conclude that the redox-separated state is formed primarily via the k_1 step followed by k_2, with k_2 rapid on the time scale of the spectroscopic experiment, $\geq 2 \times 10^8\ s^{-1}$. There was no evidence for $prPQ^{\bullet+}$ in transient absorption difference spectra of $[Boc\text{-}Lys(Ru^{II}b_2m)^{2+}\text{-}prPQ^{2+}]$, even though the MLCT emission was efficiently quenched, from which it can be inferred that $k_6 \gg k_4$ in Scheme I.[13] The redox-separated state of the PTZ dyad, $[(PTZpn^{\bullet+})\text{-}Lys(Ru^{II}b_2m)^{2+}\text{-}OCH_3]$, was observed and exhibited a lifetime of $\tau = 25$ ns ($k_3 = 4 \times 10^7\ s^{-1}$) following laser-flash photolysis. Note that the addition of a second electron-transfer step in the triad resulted in a 6-fold increase in the redox-separated state lifetime.

At its maximum appearance, the redox-separated state of the triad was formed with a quantum yield, Φ_{rss}, of 0.34 ± 0.03. This value was measured relative to the efficiency of formation of $PQ^{\bullet+}$ following oxidative quenching of $(Ru^{II}b_3)^{2+}$ by PQ^{2+}.[14] The less-than-unit efficiency in the formation of the redox-separated state must originate in the deactivational processes, k_3 and/or k_6 in Scheme I. From the high degree of emission quenching, the initial electron transfer is rapid and efficient. Neglecting the left-hand branch of Scheme I, using the values for k_1, k_3, and k_4 obtained from the model dyads, and $\Phi_{rss} = 0.34$, we calculate $k_2 \sim 2.9 \times 10^7\ s^{-1}$ ($\tau = 35$ ns). This is not consistent with the experimental observation that $prPQ^{\bullet+}$ appears with $k \sim 1.3 \times 10^8\ s^{-1}$. There may be a significant contribution from the left-hand branch of the mechanism in Scheme I or a change in rate constants in the triad compared to the model dyads.

It is possible to convert the stored energy of the redox-separated state into chemical redox energy.[15] Formation of the redox-separated state of the triad in freeze–pump–thaw–degassed CH_3CN with 532-nm excitation in the presence of both 4 mM tetramethylbenzidine (TMBD) and 3 mM benzoquinone (BQ) was followed by electron transfer from TMBD to $PTZpn^{\bullet+}$ ($k = 6 \times 10^9\ M^{-1}\ s^{-1}$) and electron transfer from $prPQ^{\bullet+}$ to BQ ($k = 1 \times 10^9\ M^{-1}\ s^{-1}$). The electron-transfer reactions, which followed pseudo-first-order kinetics, were observed by monitoring the quenching of the transient absorption of $PTZpn^{\bullet+}$ by TMBD and the quenching of $prPQ^{\bullet+}$ by BQ. In the net reaction visible light was converted into the chemical redox energy of the transient products, $TMBD^{\bullet+}$ and $BQ^{\bullet-}$.[16-17]

$$TMBD + BQ \xrightarrow[\text{lysine triad}]{h\nu_{532nm}} TMBD^{\bullet+} + BQ^{\bullet-} \quad \Delta G^\circ = 0.8\ eV$$

Using redox modules such as those described here, we are pursuing the assembly of more complex redox-active peptides.

Acknowledgment is made to the National Science Foundation (Grant CHE-8806664), the National Institute of General Medical Sciences (Grants GM32296 and GM42031), and the North Carolina Biotechnology Center (Grant 8913-ARIG-0104) for support of this research.

Supplementary Material Available: Characterization data for the compounds synthesized (3 pages). Ordering information is given on any current masthead page.

(11) Alkaitis, S. A.; Beck, G.; Grätzel, M. *J. Am. Chem. Soc.* **1975**, *97*, 5723.
(12) Watanabe, T.; Honda, K. *J. Phys. Chem.* **1982**, *86*, 2617.
(13) In order to establish that direct electron transfer between PTZpn and $prPQ^{2+}$ did not play a role, the dyad $[PTZpn\text{-}NH\text{-}prPQ^{2+}]$ was prepared.[9] This dyad showed no ground-state absorption above 375 nm. In contrast, a concentrated solution of 10-MePTZ and PQ^{2+} showed a charge-transfer absorption for the 10-MePTZ,PQ^{2+} donor–acceptor complex at 500 nm.
(14) Olmsted, J., III; Meyer, T. J. *J. Phys. Chem.* **1987**, *91*, 1649.
(15) (a) Young, R. C.; Meyer, T. J.; Whitten, D. G. *J. Am. Chem. Soc.* **1975**, *97*, 4781. (b) Nagle, J. K.; Bernstein, J. S.; Young, R. C.; Meyer, T. J. *Inorg. Chem.* **1981**, *20*, 1760.
(16) Takemoto, K.; Matsusaka, H.; Nakayama, S.; Suzuki, K.; Ooshika, Y. *Bull. Chem. Soc. Jpn.* **1968**, *41*, 764.
(17) (a) Foster, R.; Thompson, T. J. *Trans. Faraday Soc.* **1962**, *58*, 860. (b) Slifkin, M. A. *Spectrochim. Acta* **1964**, *20*, 1543.

NMR Assignment Strategy for DNA Protons through Three-Dimensional Proton–Proton Connectivities. Application to an Intramolecular DNA Triplex

Ishwar Radhakrishnan and Dinshaw Patel

Department of Biochemistry & Molecular Biophysics
Columbia University
630 West 168th Street, New York, New York 10032

Xiaolian Gao*

Department of Structural & Biophysical Chemistry
Glaxo Research Institute
Research Triangle Park, North Carolina 27709

Received July 11, 1991

Homonuclear three-dimensional (3D) proton NMR has been shown to be useful in both resonance assignments and structure determination of proteins and saccharides.[1-7] This technique is

(1) Griesinger, C.; Sørensen, O. W.; Ernst, R. R. *J. Am. Chem. Soc.* **1987**, *109*, 7227–7228.
(2) (a) Vuister, G. W.; Boelens, R.; Kaptein, R. *J. Magn. Reson.* **1988**, *80*, 176–185. (b) Vuister, G. W.; de Waard, P.; Boelens, R.; Vliegenthart, J. F. G.; Kaptein, R. *J. Am. Chem. Soc.* **1989**, *111*, 772–774. (c) Vuister, G. W.; Boelens, R.; Padilla, A.; Kleywegt, P. G.; Kaptein, R. *Biochemistry* **1990**, *29*, 1829–1839. (d) Padilla, A.; Vuister, G. W.; Boelens, R.; Kleywegt, G. J.; Cavê, A.; Parello, J.; Kaptein, R. *J. Am. Chem. Soc.* **1990**, *112*, 5024–5030. (e) Breg, J. N.; Vuister, G. W.; Kaptein, R. *J. Magn. Reson.* **1990**, *87*, 646–651.
(3) Oschkinat, H.; Cieslar, C.; Holak, T. A.; Clore, G. M.; Gronenborn, A. M. *J. Magn. Reson.* **1989**, *83*, 450–472.
(4) Oschkinat, H.; Cieslar, C.; Griesinger, C. *J. Magn. Reson.* **1990**, *86*, 453–469.
(5) Holak, T. A.; Habazettl, J.; Oschkinat, H.; Otlewski, J. *J. Am. Chem. Soc.* **1991**, *113*, 3196–3198.

0002-7863/91/1513-8542$02.50/0